UYES Ulysseus Young Explorers in Science
Volume 01 Issue 01 (2026), ISSN (Online): 2989-5642

A Graph-Driven Heuristic and Discrete Event Simulation Approach to Layout-Dependent All-Clear Building Sweeps

Yixi Xu, Shuhan Fang, Wei Geng

Ulysseus EUROPEAN UNIVERSITY

Wuhan Cogdel Cranleigh High School, Wuhan, China

Abstract

This study examines how all-clear sweeps can be planned and evaluated more efficiently during building fires. It proposes a graph-based task model that integrates heuristic generation of multiple sweep plans with discrete event simulation to evaluate multi-responder sweep execution across varying operational conditions. Experiments on two contrasting layouts show that layout shapes sweep bottlenecks. The dispersed layout benefits more from larger teams, whereas the concentrated layout benefits more from higher per-trip rescue capacity. Communication delay increases sweep time, while risk-priority routing and sensor-supported interventions improve performance. The framework provides a practical way to compare sweep strategies across different building layouts.

***Keywords*:** graph-driven heuristic, discrete event simulation, all-clear building sweep, emergency response

1 Introduction

During building fire emergencies, firefighters and other responders need to conduct an all-clear sweep, which is a critical procedure involving the systematic search and verification of every room to ensure no occupants are left behind. This process requires them to enter, search, verify, and document rooms to make sure that no occupants remain inside and that critical hazards have been identified in time (Lambert et al., 2021). In practice, however, this task is far more complicated than simply walking through each room once. Physical buildings often contain multiple floors, irregular room connections, and uneven spatial layouts, all of which affect movement, coordination, and task sequencing during emergency response (Ha & Lykotrafitis, 2012). In addition, corridor and stair capacity can create bottlenecks (Zhang et al., 2020), especially in larger or vertically organized buildings, while smoke and reduced visibility may result in lower walking speed and alter the accessibility of indoor routes (Fridolf et al., 2019). Communication also plays an important role, as incomplete or delayed information may lead to repeated checks, inefficient routing, or slow confirmation of cleared areas (Abbas & Miller, 2025).

These challenges make emergency sweep planning a complex problem of spatial organization, route design, and team coordination. Responders must cover all required locations, decide who should go where, and determine the order in

which tasks should be completed. The goal is not only to reduce total completion time, but also to clear high-risk areas as early as possible and to avoid missed or duplicated searches. Conventional evacuation studies focus on how occupants leave a building, whereas an all-clear sweep emphasizes responders' movement and task execution inside the building. Its performance depends on several operational factors, including room search time, door conditions, confirmation time, rescue capacity, congestion, and communication efficiency. Previous research on building evacuation and emergency behavior has shown that these factors can substantially influence emergency outcomes, especially in complex indoor environments (Wang et al., 2024; Wong & Lee, 2025).

Recent technological developments offer new opportunities to support building emergency response. Building information modeling (BIM)-based indoor localization and navigation systems can improve route guidance and help responders access building information more efficiently (Wong & Lee, 2025; Zhao et al., 2025). Thermal imaging can assist human detection in smoke-filled environments, and robotic platforms are increasingly being considered for reconnaissance, search, and operations in hazardous areas where direct human access may be unsafe (Tsai et al., 2022). At the same time, recent quantitative work suggests that the actual benefits of navigation and information-sharing technologies depend on how they interact with participant behavior and response collaboration, meaning that their value should be tested in a structured and reproducible way rather than assumed in advance (Wong & Lee, 2025).

To address these issues, this study proposes a graph-driven multi-plan heuristic (GMH) and discrete event simulation (DES)-based building sweep model (BSM), hereafter referred to as the GMH-DES-BSM framework, for all-clear building sweeps. In the framework, floor plans are first represented as graphs in which rooms, hallways, exits, and traversable connections are linked with task-related attributes. A heuristic procedure then generates multiple feasible sweep plans for responders, and a DES module evaluates their realized performance under passage-capacity constraints and dynamic execution delays.

The contribution of this study is threefold. First, it develops a GMH and DES-based evaluation framework that links building topology, task allocation, rescue-return movement, and congestion-aware execution. Second, it reframes all-clear building sweeps as an integrated responder-centered task rather than as a conventional occupant evacuation problem. Third, it identifies layout-dependent sweep mechanisms, showing that different building layouts require different combinations of team size, rescue capacity, communication efficiency, and sensor-supported intervention.

2 Literature review

2.1 Building evacuation and indoor movement under hazardous conditions

Existing research on building emergencies is largely grounded in mature evacuation-modeling frameworks and focuses on occupants' perception, decision-making, movement, and evacuation under hazardous conditions. Early studies of building evacuation evolved beyond corridor-capacity analysis toward multi-layered frameworks that jointly represent individual behavior, spatial constraints, and scenario uncertainty (Kuligowski et al., 2010). Building on this foundation, subsequent work has shown that internal spatial connectivity is a key determinant of movement efficiency and evacuation organization. In particular, the coupling among rooms, floors, stairways, corridors, exits, and vertical

circulation systems can alter crowd distribution, local congestion patterns, and total evacuation time, such that identical population sizes may exhibit markedly different evacuation responses under different building layouts (Ha & Lykotrafitis, 2012; Ronchi & Nilsson, 2014). At the same time, the dynamic evolution of hazardous environments further increases model complexity. Smoke density, reduced visibility, and fire development not only lower walking speed but also affect orientation, route choice, and avoidance behavior, thereby transforming evacuation from a relatively stable flow problem into a dynamic process shaped by environmental feedback (Fridolf et al., 2013). Behavioral studies further emphasize that occupants' responses in fires are not determined solely by shortest-path principles, but are also closely related to risk perception, information interpretation, familiarity, herding behavior, and pre-movement time. Thus, even under the same building geometry, different population compositions and information conditions may lead to substantially different behavioral patterns (Kobes et al., 2010; Lin et al., 2020). Overall, existing studies have provided valuable insights into how building form, hazardous conditions, and individual behavior influence indoor movement. Their primary concern, however, remains how occupants leave a building, rather than how responders enter it and complete an all-clear sweep.

2.2 Responder search verification and team coordination

A related research stream shifts the focus from occupants to responders, emphasizing their search, verification, and rescue behaviors under low visibility, high time pressure, and complex spatial conditions. Empirical studies have quantified responders' movement characteristics in indoor fire environments, showing that crawling speeds under poor visibility differ markedly from the upright walking speeds commonly assumed in evacuation research (Lambert et al., 2021; Muhdi et al., 2009). At the methodological level, coverage, routing, and scheduling problems have been addressed primarily through network optimization and operations research. Network-based studies have incorporated exit allocation, route conflict, capacity constraints, visit order, and path generation into unified frameworks, thereby providing a methodological basis for responder task allocation and route organization (Chalmet et al., 1982; García-Ojeda et al., 2013; Vermuyten et al., 2016). Other studies conceptualize emergency performance as the outcome of interactions among humans, buildings, and emergency systems, highlighting the influence of information flow, real-time communication, environmental feedback, and group interaction on individual decisions and collective coordination. Under multi-agent parallel operations, communication delay and information distortion may trigger repeated searches, missed verification, and local congestion, thereby substantially reducing response efficiency (Templeton et al., 2024; Zhu et al., 2020). Overall, although existing studies have laid important foundations for building emergency search from the perspectives of empirical measurement, path optimization, and interaction mechanisms, they remain insufficiently integrated for the specific task of all-clear sweeps.

2.3 Sensor and digitally supported emergency response

Recent advances in sensor and digital technologies are reshaping building emergency response, shifting it from experience-based, verbally coordinated practice toward digitally supported decision-making grounded in spatial data, real-time sensing, and multi-party information sharing. Prior studies show that the integration of BIM and indoor localization can support position identification and route inference, while indoor navigation systems combining voice interaction, inertial sensing, and multi-user collaboration further extend digital spatial representation from static modeling to real-time operational support (Li et al.,

2014; Wong et al., 2022). At the same time, thermal imaging, inertial sensing, computer vision, and multi-source localization provide faster situational input under low visibility, smoke occlusion, and complex spatial conditions. In particular, deep-learning-based human detection using thermal imaging and BIM computer vision frameworks for local safety assessment both demonstrate the potential to improve target recognition and environmental understanding (Deng et al., 2021; Tsai et al., 2022). Multi-user information-sharing platforms further elevate individual responders' localization, navigation, and sensing capabilities to team-level real-time coordination, although their effectiveness remains constrained by human behavior and coordination patterns (Wong & Lee, 2023, 2025). In parallel, robots are increasingly used for fire-ground reconnaissance and forward search in hazardous zones (Wang et al., 2024). However, existing studies remain largely focused on the performance of individual technologies and rarely compare, within a unified task framework, how different technology combinations affect all-clear sweep efficiency.

2.4 Gap analysis

Existing studies have focused primarily on occupant evacuation, responder search behavior, or support from individual digital technologies, while treating all-clear sweeps as an integrated task only to a limited extent. More specifically, spatial coverage, room verification, exit return, team allocation, and dynamic risk are often examined in isolation rather than within a unified analytical framework. Likewise, the combined effects of building layout, team size, and technology configuration on sweep efficiency remain insufficiently compared. Therefore, the key gap is not simply the lack of another routing algorithm, but the absence of a task-level modeling framework that can connect building topology, responder assignment, room verification, rescue-return movement, and congestion-aware execution within the same analytical process. This study addresses this gap by proposing the GMH-DES-BSM framework, which generates multiple time-efficient sweep plans on a graph representation of the building and then evaluates their realized performance through DES under passage-capacity constraints and operational uncertainties.

3 Methodology

This study proposes the GMH-DES-BSM framework to investigate all-clear sweep operations under building fire scenarios. The research framework is shown in Figure 1. The proposed framework is structured into four sequential phases.
First, in the materials preparation and graph construction phase, two contrasting public-building layouts are modeled from floor plans, node attributes, and basic assumptions, and are abstracted into a graph $G(V, E)$ as the model input.
Second, in the GMH-based plan generation phase, an earliest-available-first multi-plan heuristic is then used to generate task-allocation and routing schemes for multiple firefighters.

Third, in the DES-based execution and evaluation phase, the studied plans are evaluated in a DES module, which captures their actual execution under passage-capacity constraints and dynamic interactions, thereby identifying the best-performing team configurations and sweep plans for different building layouts.
Finally, in the scenario comparison phase, additional scenarios incorporating communication delay, risk-priority routing, and sensor-supported interventions are examined to compare sweep efficiency across layouts and operational conditions.

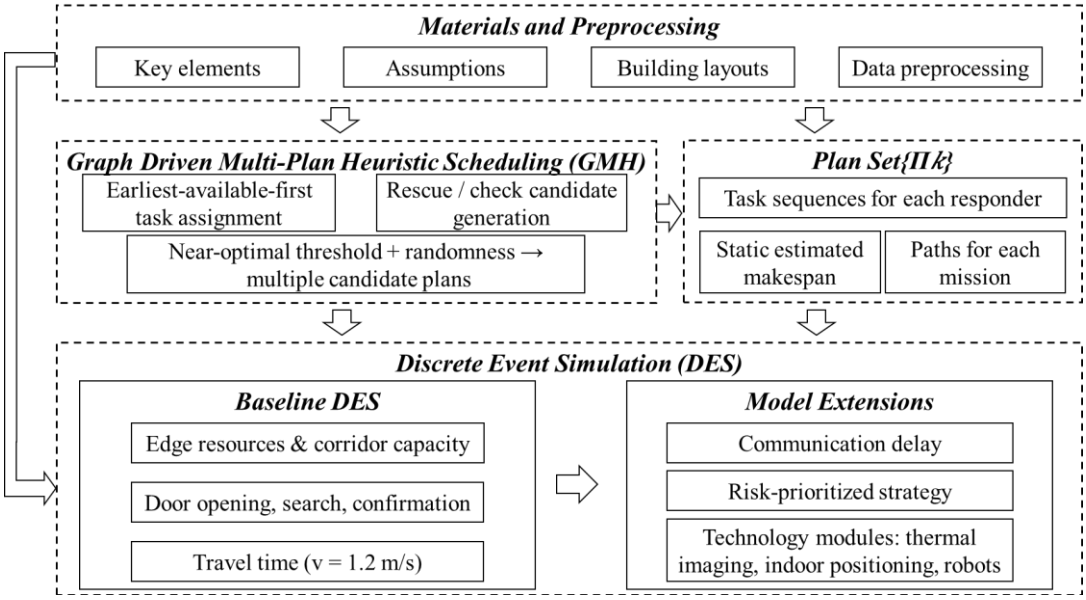

Figure 1.
Research framework of GMH-DES-BSM

The primary objective of this study is to develop a simulation framework for all-clear sweeps in buildings and to evaluate how building layout, team configuration, communication delay, risk-priority routing, and sensor deployment affect sweep efficiency. The framework covers the complete process of all-clear sweeps, including firefighters' entry, search, verification, rescue, and return when necessary, with total completion time used as the primary performance metric. On this basis, the study further compares the key factors shaping sweep efficiency across different building types, with the aim of identifying representative organizational patterns and resource-allocation principles for all-clear operations.

3.1 Materials and preprocessing

To support these objectives, two contrasting public-building layouts were selected: a two-story children's daycare center and a three-story museum. These two cases were chosen not to provide an exhaustive typology of public buildings, but to represent two distinct spatial and operational patterns that are highly relevant to all-clear sweeps. The daycare center represents a dispersed multi-room layout, where occupants are distributed across many relatively small and functionally separated rooms. Such a layout requires broad room-by-room coverage, frequent verification, and coordination among multiple firefighters moving through shared corridors. In contrast, the museum represents a more concentrated multi-floor layout, where occupants are mainly clustered in larger exhibition areas and movement is shaped by vertical circulation and repeated return trips from high-demand spaces. Therefore, the two building layouts differ in room subdivision, occupant distribution, circulation structure, and expected sweep bottlenecks. Comparing them allows the proposed framework to examine whether sweep efficiency is primarily constrained by parallel spatial coverage or by rescue throughput from concentrated demand locations.

3.1.1 Building layout 1. Children's daycare center

Building layout 1 is a two-story children's daycare center (Figure 2). Its dimensions are set according to typical classroom building standards (for example, a 30-student classroom has a minimum floor area of approximately 50.2 m², according to Classroom Space Utilization Guidelines (2024)). We convert the floor plan into a graph whose nodes and edges represent rooms, hallways, and exits. The number

of occupants assigned to each room or hallway node ranges from 0 to 30. Classrooms and similar spaces are modeled as furnished. We assign heterogeneous risk levels to different locations: classrooms are given the highest risk level 4, because they may contain the largest number of occupants; hallway cells immediately outside classroom doors are assigned risk level 3 to reflect their importance for movement and potential congestion; ordinary hallway segments are set to risk level 2; and hallway cells near exits are assigned the lowest risk level 1.

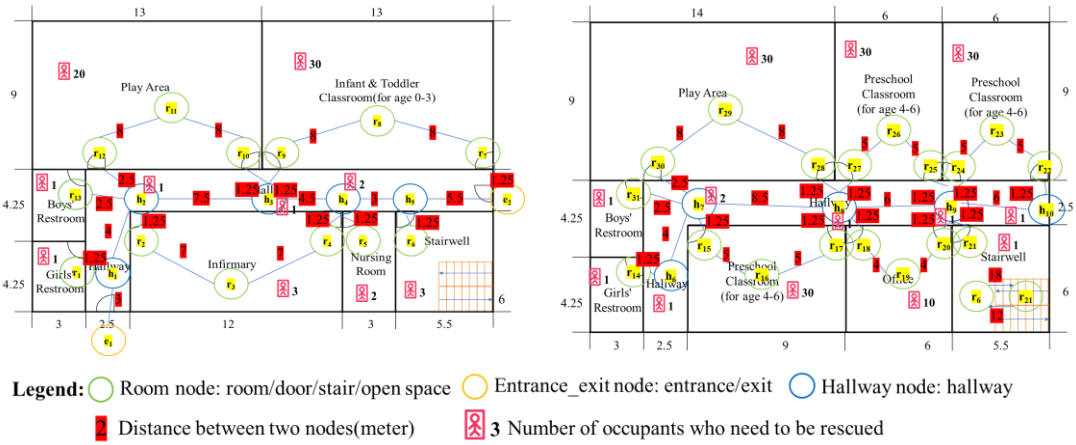

(a) first floor (b) second floor

Figure 2.

Building layout 1: children's daycare center floor plan.

3.1.2 Building layout 2. Museum

Building layout 2 is the Paul Revere Museum of Discovery and Innovation (Paul Revere Memorial Museum, 2021) (Figure 3), a three-story museum with a more vertically organized layout. The configuration of this building layout follows the same principles as building layout 1, with the main difference that occupants are highly concentrated in the exhibition areas, which are therefore assigned the highest risk level.

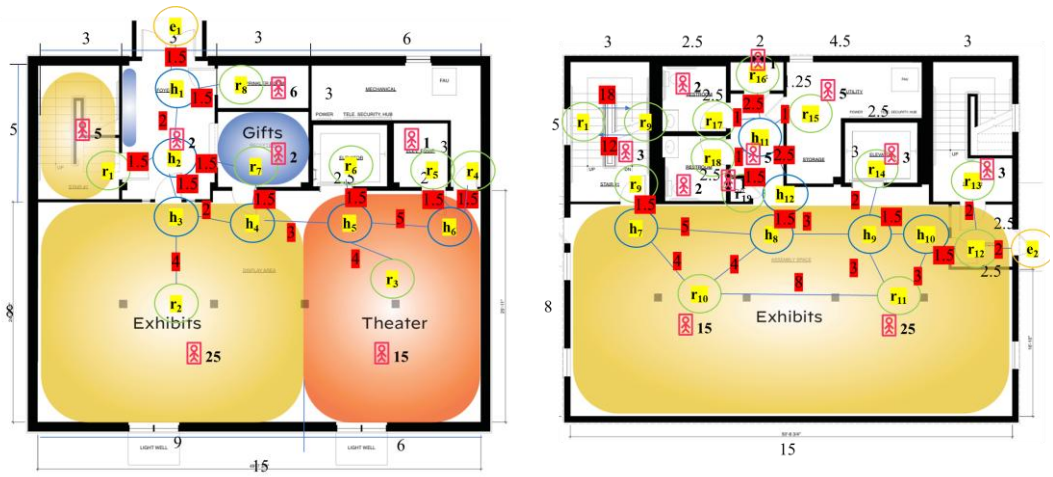

(a) first floor (b) second floor

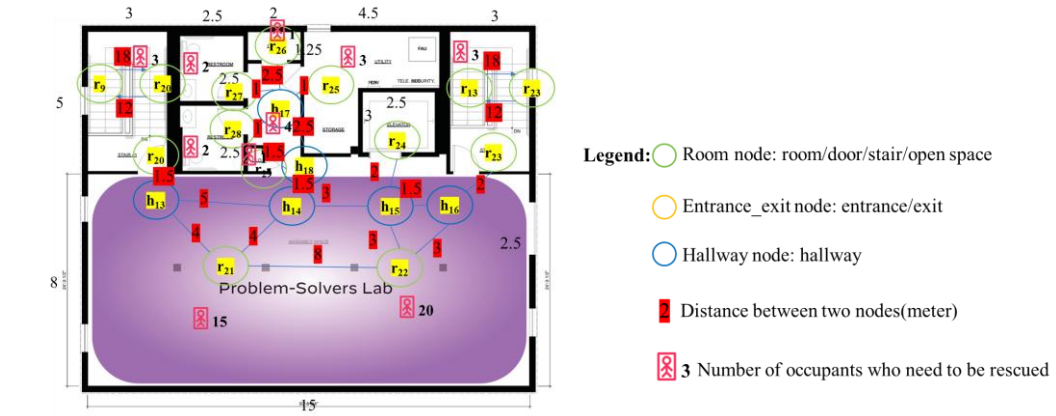

(c) third floor

Figure 3.
Building layout 2: floor plan of Paul Revere Museum of Discovery and Innovation.

3.1.3 Graph representation and preprocessing

After defining the two building layouts, their floor plans were represented as a graph $G(V,E)$. Nodes denote rooms, hallway junctions, and exits, and are associated with attributes such as room function, occupant count, door state, and risk level (Table 1). Edges represent traversable spatial connections and are assigned attributes including distance and width (Table 2). In this graph representation, room and hallway nodes serve not only as spatial units but also as task-bearing units. A rescue task is triggered when occupants remain at a node, whereas a check task is triggered when the required number of inspections has not yet been completed. Exit nodes represent the entry and return locations for firefighters. Based on this unified representation, the heuristic module performs task allocation and path generation on the graph structure, while the DES module further simulates dynamic execution.

Table 1.
Attributes of nodes.

Attribute	Field type	Values	Description
type	string	room, hallway, exit_entrance	Room: represents an enclosed room separated from other spaces. Exit_entrance: represents an entry/exit point, used as the firefighters' access point and the evacuation exit. Hallway: represents door–hallway junctions or open lobby areas.
id	string	such as r1, h1, e1,	Unique identifier of the node
if_furniture	int	0,1	Layout indicator: 0 = unfurnished, 1 = furnished
occupant_num	int	0,1,2...	Number of occupants in the room awaiting rescue
area	float	such as 15.0	Area (m^2)
door_state	int	0,1,2	Door status: 0 = locked, 1 = open, 2 = locked with a certain probability
check_num	int	1,2,3...	Required number of checks for this location
current_check_num	int	0,1,2,3...	Current number of completed checks (initially 0)
risk_level	int	1,2,3,4	Risk level determined by the room type

Table 2.
The structure and attributes of edges.

Edge attribute	Field type	Description
node1_id	string	id of the head node connected by the edge
node2_id	string	id of the tail node connected by the edge
distance	float	Length of the hallway segment
width	float	Width of the hallway

The basic graph configurations for the two building layouts are summarized in Table 3.

Table 3.
The basic graph configurations for the two building layouts.

Building layout	Node count	Edge count	Total area(m^2)	Total occupants
1. Children's daycare center	43	100	910	203
2. Museum	47	112	630	177

3.2 Heuristic multi-plan generation: task assignment and route design

This section presents a heuristic procedure for generating candidate sweep plans for multiple firefighters. The procedure determines (1) which nodes are assigned to which firefighter, (2) in what order each firefighter visits these nodes, and (3) how multiple candidate plans can be produced under the same initial conditions for subsequent simulation-based evaluation. Rather than seeking a strict global optimum, the heuristic aims to generate a set of computationally efficient and near-optimal sweep plans that can later be compared within the DES framework. The method is based on the following idea: given a static graph representation of the building and the task requirements associated with each node, each firefighter is treated as an individual responder characterized by a current position and an accumulated occupied time. A coordinated multi-firefighter sweep plan is then constructed by iteratively assigning the most suitable next task to the firefighter who becomes available first.

3.2.1 Node tasks and firefighter states

For each room or hallway node i, let n_i denote the number of occupants requiring rescue, c_i^{req} denote the required number of checks, and c_i^{cur} denote the number of checks already completed. We define two binary task indicators: I_i^R for a rescue task R_i, and I_i^C for a check task C_i. A firefighter is denoted by $f \in \mathcal{F}$, where $\mathcal{F}$ is the set of available firefighters. These quantities determine whether node i still has unfinished tasks.

A rescue task is required when occupants remain at node i:

$$I_i^R = \begin{cases} 1, n_i > 0 \\ 0, n_i = 0 \end{cases} \tag{1}$$

A check task is required when the completed number of checks is smaller than the required number:

$$I_i^C = \begin{cases} 1, c_i^{cur} < c_i^{req} \\ 0, c_i^{cur} \geq c_i^{req} \end{cases} \tag{2}$$

Thus, a node may require rescue, inspection, both, or neither. When both conditions hold, rescue is prioritized. In this study, a completed rescue is also counted as one completed check because the firefighter must physically enter and verify the node during rescue.

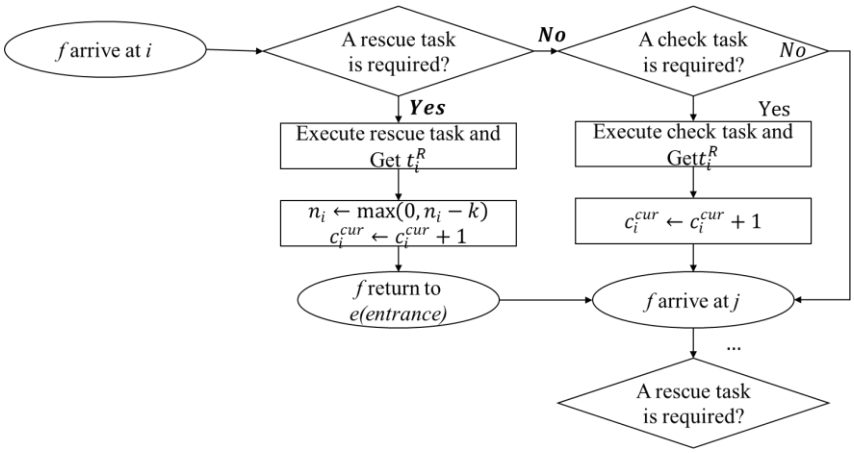

Figure 4.
Schematic illustration of node-level task states and priority rules.

Figure 4 schematically summarizes the node-level task states. It is intended as a conceptual illustration of how rescue, check, and transit states are distinguished, rather than as a full process diagram. When a firefighter arrives at node i, the indoor operation time depends on the task type and node attributes. For rescue tasks, following Lambert et al. (2021), the indoor operation time is determined by room area, furniture condition, and the number of trapped occupants:

$$t_i^R = \begin{cases} (0.352 + n_i \cdot 0.066) \cdot A_i, \text{if node } i \text{ is furnished and occupied} \\ (0.184 + n_i \cdot 0.066) \cdot A_i, \text{if node } i \text{ is unfurnished and occupied} \end{cases} \quad (3)$$

where A_i is the area of node i, n_i is the number of remaining occupants at node i, and t_i^R is the indoor operation time and is measured in minutes. It is subsequently converted into seconds, and an additional confirmation time t_{conf} is added:

$$\tilde{t_i^R} = 60 t_i^R + t_{conf} \quad (4)$$

where $\tilde{t_i^R}$ is the total rescue-operation time in seconds and t_{conf} is the confirmation time.

In each rescue task, the firefighter rescues up to k occupants, where k denotes the rescue capacity per trip. The node state is updated as:

$$n_i \leftarrow \max(0, n_i - k) \quad (5)$$

$$c_i^{cur} \leftarrow c_i^{cur} + 1 \quad (6)$$

After completing the rescue, the firefighter must escort the rescued occupants to the nearest exit before receiving the next assignment.

For check tasks, the indoor operation time is defined as:

$$t_i^C = \begin{cases} 0.352\ A_i, \text{if node } i \text{ is furnished and unoccupied} \\ 0.184\ A_i, \text{if node } i \text{ is unfurnished and unoccupied} \end{cases} \quad (7)$$

where t_i^C is the indoor check operation time at node i, and the total check time is

$$\widetilde{t_i^C} = 60t_i^C + t_{conf} \tag{8}$$

where $\widetilde{t_i^C}$ is the total check-operation time in seconds. In this case, only the inspection state is updated (Equation (6)).

3.2.2 Iterative heuristic task assignment and route design

At any step of the heuristic procedure, firefighter f is characterized by two state variables: the current node p_f and the accumulated occupied time τ_f. Let $\mathcal{E}$ denote the set of exits. For any pair of nodes (u, v), the shortest-path travel time is defined as:

$$\mathrm{T}(u, v) = \frac{d(u, v)}{v_0} \tag{9}$$

where $T(u, v)$ is the travel time from node u to node v, $\mathrm{d}(u, v)$ is the shortest-path length between nodes u and v, and v_0 is the baseline walking speed of firefighters. The time required to return from node i to its nearest exit is

$$T_{back}(i) = \min_{e \in \mathcal{E}} T\,(i, e) \tag{10}$$

where $T_{back}(i)$ is the minimum return time from node i to an exit, and e denotes an exit node in $\mathcal{E}$. The heuristic assignment process is performed iteratively in an offline manner until all rescue and check requirements have been satisfied.

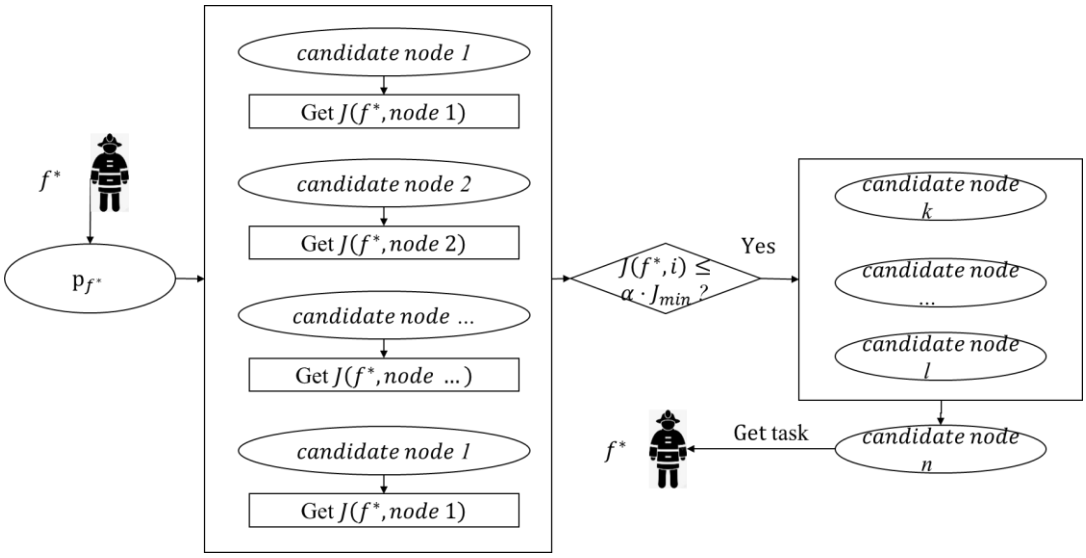

Figure 5.
Conceptual illustration of the iterative task assignment procedure.

Figure 5 conceptually illustrates the iterative assignment process, including firefighter selection, candidate task evaluation, near-optimal set construction, and state updating.

At each iteration, the firefighter to be assigned next is selected as the one who becomes available earliest:

$$f^* = \arg\min_{f \in \mathcal{F}} \tau_f \tag{11}$$

where f^* is the selected firefighter, $\mathcal{F}$ denotes the set of all firefighters.
For the selected firefighter f^*, whose current position is $s = p_{f^*}$, candidate tasks are enumerated over all nodes with unfinished requirements. If node i requires rescue, the total time cost is

$$C_i^R(f^*) = \mathrm{T}(s,i) + \widetilde{t_i^R} + T_{back}(i) \tag{12}$$

where $C_i^R(f^*)$ is the total cost of assigning a rescue task at node i to firefighter f^*. The three terms $T(s,i), \widetilde{t_i^R}, T_{back}(i)$ represent outbound travel, indoor rescue plus confirmation, and return-to-exit time, respectively.

If node i requires only inspection, the total time cost is

$$C_i^C(f^*) = \mathrm{T}(s,i) + \widetilde{t_i^C} \tag{13}$$

where $C_i^C(f^*)$ is the total cost of assigning a check task at node i to firefighter f^*, and $\widetilde{t_i^C}$ is the total check-operation time at node i.

For each candidate node i, the heuristic score is defined by the corresponding task-dependent time cost:

$$J_i(f^*) = \begin{cases} C_i^R(f^*), \text{ if } I_i^R = 1 \\ C_i^C(f^*), \text{ if } I_i^R = 0 \text{ and } I_i^C = 1 \end{cases} \tag{14}$$

where $J_i(f^*)$ is the heuristic score of assigning node i to firefighter f^*. Rescue tasks are evaluated first because rescue is prioritized when both rescue and check requirements exist at the same node.

Let $\mathcal{L}$ denote the set of candidate nodes. The best score is

$$J_{min} = \min_{i \in \mathcal{L}} J_i\,(f^*) \tag{15}$$

where J_{min} is the smallest heuristic score among all candidate nodes for the selected firefighter.

To avoid producing only a single purely greedy solution, an approximate-optimal threshold $\alpha \geq 1$ is introduced. All candidate nodes satisfying $J_i(f^*) \leq \alpha J_{min}$ are included in a near-optimal candidate set. One node i^* is then selected uniformly at random from this set and assigned to firefighter f^*. This design allows multiple structurally different, yet time-efficient, plans to be generated under identical initial conditions.

Once the target node i^* and the corresponding task type have been selected, a task record is created for firefighter f^*, including the starting node, target node, outbound path, task type, planned start time, and planned completion time. The system state is then updated.
For the firefighter state,

$$\tau_{f^*} \leftarrow \tau_{f^*} + J_{i^*}(f^*) \tag{16}$$

$$p_{f^*} \leftarrow \begin{cases} e^*(i^*), \text{ if node } i^* \text{ is assigned a rescue task} \\ i^*, \text{ if node } i^* \text{ is assigned a check task} \end{cases} \tag{17}$$

where τ_{f^*} denotes the accumulated occupied time of firefighter f^*, i^* denotes the selected target node, p_{f^*} denotes the current position of firefighter f^*, $e^*(i^*)$ denotes the exit nearest to node i^*.

For the node state, the update follows the rescue or check rules defined above. Through iteration, rescue and check tasks are gradually partitioned among firefighters. In this way, the heuristic combines an earliest-available-first rule with local time-cost minimization to construct a coordinated multi-firefighter sweep plan.

3.2.3 Generation of multiple candidate plans

To obtain a set of candidate plans for subsequent DES-based evaluation, the heuristic procedure is repeated multiple times while keeping the initial graph structure and node states unchanged. Different random seeds are used so that, in each run, the target node is differently selected from the near-optimal candidate set.

As a result, the model produces a family of candidate sweep plans $\{\Pi_k\}_{k=1}^{K}$, where each plan Π_k contains the task sequence of every firefighter, the assigned target nodes, the path information, and the static predicted completion time (heuristic makespan). These plans are subsequently evaluated within the DES framework to examine their actual performance under congestion, resource competition, and other execution-related constraints. In this way, the heuristic module serves as the plan-generation component of the overall modeling framework, while DES provides the dynamic validation and comparison of candidate plans.

3.3 DES-based execution and evaluation

The heuristic procedure described in Section 3.2 generates a family of candidate sweep plans $\{\Pi_k\}_{k=1}^{K}$, each of which specifies the task sequence, target nodes, and planned routes for all firefighters under static assumptions. However, these plans do not explicitly account for dynamic interactions during execution, such as hallway capacity limits, waiting caused by concurrent movement, or scenario-dependent operational adjustments. To address this issue, the candidate plans are further evaluated in a DES framework. The DES module dynamically replays the execution of each plan along the time axis and produces a more realistic estimate of total sweep time under spatial constraints and operational conditions.

3.3.1 Simulation entities and environment

In the DES framework, firefighters are treated as active entities that execute the task sequences generated by the heuristic module. The building graph $G(V, E)$ provides the simulation environment, where nodes represent rooms, hallway junctions, and exits, and edges represent traversable spatial connections. Each firefighter $f \in \mathcal{F}$ is characterized by a current position $p_f(t)$, a current task status, and a time-dependent execution history.

The simulation environment contains two types of constraints. First, node-level operations inherit the rescue and check requirements defined in Section 3.2. A firefighter arriving at node i performs either a rescue operation or a check operation, depending on the node state and the assigned task. Second, edge-level movement is constrained by shared passage resources. Since multiple firefighters may travel simultaneously, hallway segments are modeled as limited-capacity resources rather than unconstrained links. This allows the DES framework to capture waiting, local conflict, and movement delay during plan execution.

Accordingly, the DES module does not generate new plans by itself. Instead, it serves as a dynamic execution layer that evaluates whether a candidate plan

remains efficient once interactions among firefighters and shared passage resources are taken into account.

3.3.2 Event execution and temporal updating

For each firefighter f, the heuristic module provides an ordered task list:

$$\mathcal{M}_f = \{M_{f,1}, M_{f,2}, \dots, M_{f,L_f}\} \tag{18}$$

where L_f is the number of tasks assigned to firefighter f. Each task $M_{f,\ell}$ contains a task type (rescue or check), a starting node, a target node, and an outbound path generated in the heuristic stage. For rescue tasks, a return path to the nearest exit is also specified.

Task execution in the DES framework consists of four sequential stages:

(1) Task start.
The $\ell - th$ task assigned to firefighter f can start only when both conditions are satisfied: the firefighter has completed the previous task, and the planned task order allows the new task to begin. In other words, DES respects the task sequence generated by the heuristic but updates the actual task start time according to realized execution delays.

(2) Outbound movement.
Once a task starts, the firefighter travels from the current position to the target node along the predetermined shortest path. The actual movement time depends not only on path length but also on whether passage capacity is available on each edge at the time of entry. If the target edge is fully occupied, the firefighter must wait before proceeding.

(3) Node-level operation.
After arriving at the target node, the firefighter performs the assigned rescue or check operation. The operation time follows the task-dependent formulation given in Section 3.2. Rescue tasks include both indoor search/rescue time and confirmation time, and they also update the node-level rescue and inspection state. Check tasks update only the inspection state.

(4) Return movement.
If the task is a rescue task, the firefighter must escort the rescued occupants to the nearest exit before receiving the next assignment. For check tasks, no return-to-exit movement is required unless the check is the final task in the firefighter's task list and the simulation setting requires the firefighter to end at an exit. In this way, the DES module distinguishes between direct task chaining and task completion with exit return.

For each candidate plan, the simulation proceeds event by event until all tasks assigned in that plan have been executed. The main advantage of this mechanism is that the actual sweep process is evaluated under dynamic timing, rather than under the static assumption that all movements occur without interference.

3.3.3 Passage resource constraints and dynamic interactions

A key purpose of the DES module is to represent dynamic interactions among firefighters when they share the same circulation space. To achieve this, each edge $(u, v) \in E$ is assigned a capacity value that reflects the maximum number of firefighters that can traverse the edge simultaneously. Let w_{uv} denote the width

of edge (u, v), w_0 the width required for one firefighter to pass, and c_{max} an upper bound on edge capacity. The capacity of edge (u, v) is defined as:

$$c_{uv} = \min\left(c_{max}, \left\lfloor \frac{w_{uv}}{w_0} \right\rfloor\right) \tag{19}$$

Under this constraint, a firefighter may enter an edge (u, v) only if the number of firefighters currently traversing that edge is smaller than c_{uv}. Otherwise, the firefighter must wait at the edge entrance until capacity becomes available. This first-come, first-served resource mechanism allows the DES to capture congestion and queueing effects caused by simultaneous task execution.

Compared with the heuristic stage, the DES framework therefore produces a realized movement time that may be longer than the nominal shortest-path travel time. This difference is particularly important for layouts with narrow corridors, frequent path overlap, or strong local concentration of tasks. Because the retained results of this study focus on comparisons between building layouts and on the effect of selected operational conditions, incorporating such dynamic interactions is essential for moving from static planning to realistic execution-based evaluation.

3.3.4 Evaluation metrics

The DES framework evaluates each candidate plan Π_k by the realized total sweep time, defined as the time at which all assigned tasks have been completed:

$$T_k^{DES} = \max_{f \in \mathcal{F}} F_{f,L_f} \tag{20}$$

where F_{f,L_f} denotes the completion time of the last task assigned to firefighter f. This quantity is the primary performance indicator in this study and is referred to as the total sweep time.

To quantify the discrepancy between the static heuristic estimate and the dynamically executed plan, we further define the execution delay of plan Π_k as:

$$\Delta T_k = T_k^{DES} - T_k^{H} \tag{21}$$

where T_k^H is the heuristic makespan predicted in Section 3.2. A larger ΔT_k indicates that the static plan is more strongly affected by dynamic interactions during execution.

For scenario comparison, the best-performing plan under a given setting is identified as the one with the smallest realized sweep time. This metric is used consistently in the retained results to compare the two building layouts under baseline conditions and to evaluate how communication delay, risk-priority routing, and sensor-supported interventions influence plan performance. When intervention scenarios are compared with their corresponding baseline settings, the relative improvement is measured by the percentage reduction in total sweep time.

In this way, the DES module plays two roles in the overall framework. First, it provides a dynamic validation layer for the candidate plans generated by the heuristic module. Second, it establishes a unified evaluation basis for comparing different layouts and scenario settings under a consistent execution model.

3.4 Software implementation

The proposed GMH-DES-BSM framework was implemented and tested in Python 3.10 using Visual Studio Code 1.120 as the integrated development environment. Python was used to program the graph-driven heuristic procedure, execute the discrete event simulation, conduct the scenario-based experiments, and generate the figures and the table presented in the Results and Discussion section. Python was selected because it provides flexible support for graph-based computation, iterative algorithm implementation, event-based simulation, and reproducible batch experiments. Visual Studio Code was used for code development, debugging, and experimental script management because it provides an integrated and lightweight environment for editing, running, and managing Python scripts.

4 Results and Discussion

4.1 Experimental settings

The experiments were designed to support four groups of comparisons: baseline layout comparison, communication delay, risk-priority routing, and sensor-supported intervention. All simulations were conducted on the two representative building layouts introduced in Section 3.1, namely the children's daycare center and the museum.

For the baseline experiments, the firefighters' walking speed was set to $v_0 = 1.2$ m/s (Chen et al., 2025), and the confirmation time was set to $t_{conf} = 10\ s$ (Beattie et al., 2022). The number of firefighters ranged from 1 to 100, and the rescue capacity per trip k ranged from 1 to 5 persons. Door conditions followed the node settings defined in Section 3.1. Passage constraints in the DES module were controlled by the per-person required width $w_0 = 0.6$ m (Fruin, 1971) and the maximum edge capacity $c_{max} = 5$. Under these settings, the model identified the best-performing plan for each layout by the smallest realized sweep time.

For the communication-delay experiments, an additional delay term δ_{com} was added to t_{conf} to represent reporting and instruction delays after each task. The value of δ_{com} varied from 1 s to 30 s, while all other parameters remained unchanged.

For the risk-priority experiments, each node i was assigned a priority score:

$$R_i = n_i r_i \tag{22}$$

where R_i represents the priority score of node i, n_i is the number of remaining occupants and r_i is the predefined risk level of the node. This setting allowed the heuristic to favor tasks with higher urgency while retaining the same DES evaluation procedure.

For the sensor-supported experiments, three intervention scenarios were considered: thermal infrared imaging (IR), indoor positioning and navigation support (POS), and robotic pre-inspection (ROB), together with a combined scenario (IR+POS+ROB). IR was modeled as a reduction in node-level operation time, POS as an increase in effective walking speed, and ROB as a reduction in unnecessary checks at unoccupied nodes. All intervention scenarios were evaluated under the same baseline settings so that their effects on realized sweep time could be directly compared.

4.2 Baseline differences between the two layouts

To provide a common reference for the subsequent analyses, we first compared the two representative building layouts under the baseline setting described in Section 4.1, without additional communication delay, risk-priority routing, or sensor-supported intervention. The goal was to identify the best-performing sweep configuration for each layout and to examine how differences in spatial organization and occupant distribution shape sweep efficiency.

Figure 6 shows the heuristic results across different combinations of firefighter number and rescue capacity for the children's daycare center and the museum. In both layouts, total sweep time decreases as response resources increase, but the reduction is clearly nonlinear. The marginal benefit is substantial at low resource levels and gradually diminishes as the system approaches a near-saturated state. This pattern indicates that sweep performance is constrained not only by the amount of available manpower but also by the underlying spatial structure and task distribution.

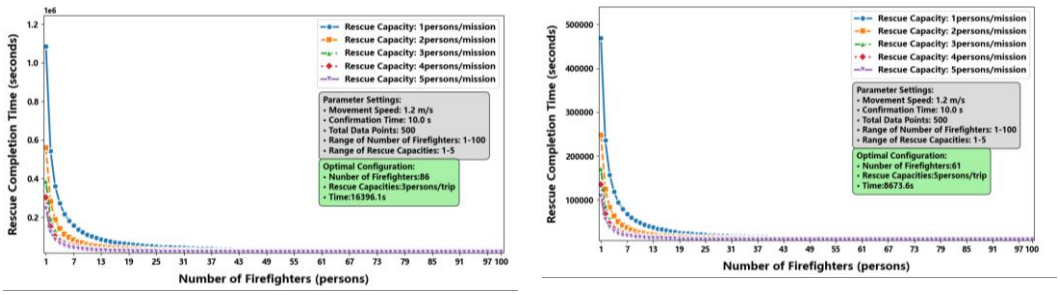

(a) Daycare center (b) Museum

Figure 6.

Total sweep time under different team sizes and rescue capacities in the ideal cases.

When the candidate plans are evaluated in the DES framework, the two layouts exhibit markedly different optimal configurations. For the daycare center, the best-performing baseline configuration is 86 firefighters with a rescue capacity of 3 persons per trip, yielding a realized total sweep time of approximately 16396.2 s. For the museum, the DES-based best-performing configuration is 59 firefighters with a rescue capacity of 5 persons per trip, yielding a realized total sweep time of approximately 8683.6 s. As shown in Figure 7 and Table 4, the DES-based completion time is slightly higher than the heuristic estimate in both cases, but the magnitude of the delay differs: the average delay is about 152.5 s in the daycare center, compared with 47.7 s in the museum.

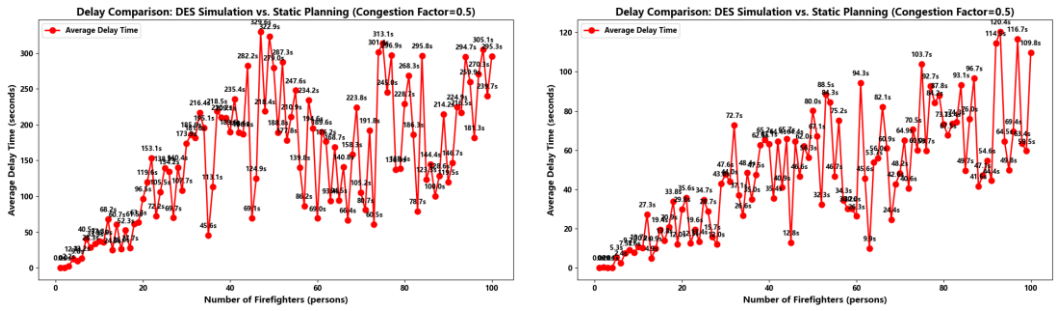

(a) Daycare center (b) Museum

Figure 7.

Delay between congestion-aware DES rescue time and the ideal (uncongested) rescue time.

Table 4.
Comparison of optimal configurations in the ideal cases and the hallway-congestion cases.

Building layout	Ideal heuristic					DES					Average delay
	Ft	St	At	Bnf	Brc	Ft	St	At	Bnf	Brc	
Daycare center	16396.1	1084212	35564	86	3	16396.2	1084212.2	35716.5	86	3	152.5
Museum	8673.6	469713	16604.5	61	5	8683.6	469713.4	16652.2	59	5	47.7

Note: Ft denotes the fastest time; St denotes the slowest time; At denotes the average time;

Bnf denotes the best number of firefighters; Brc denotes the best rescue capacity.

These differences reflect two distinct sweep mechanisms. The daycare center represents a dispersed, multi-room layout in which occupants are distributed across many separate rooms. Under this pattern, sweep efficiency depends strongly on parallel room-level coverage, so increasing team size produces a greater benefit than increasing rescue capacity alone. By contrast, the museum exhibits a more concentrated layout, in which occupants are clustered in a smaller number of key spaces. In this case, the dominant bottleneck is repeated transport from high-demand locations, making rescue capacity more influential than further increases in team size.

The larger DES delay observed in the daycare center further suggests that dispersed layouts are more sensitive to dynamic movement interactions on shared passages. Overall, the baseline comparison shows that building layout fundamentally shapes the most effective sweep strategy: the daycare center is more sensitive to team size, whereas the museum is more sensitive to per-trip rescue capacity. This distinction provides the basis for the following analyses of communication delay, risk-priority routing, and sensor-supported intervention.

4.3 Effects of communication delay

To examine the effect of communication inefficiency, we added an extra delay term to the confirmation time after each rescue or check task and re-evaluated the best baseline configurations of the two layouts. As shown in Figure 8, total sweep time increases approximately linearly with communication delay in both layouts, but the sensitivity differs: under the optimal configurations, each additional second of communication delay increases total sweep time by about 1 s in the daycare center and about 2 s in the museum.

This difference is mainly related to how the delay propagates through the critical execution path. In the daycare center, the sweep task is distributed across many rooms and a larger firefighter team, so task execution is highly parallel. Under this structure, many confirmation delays occur simultaneously across firefighters and are partially absorbed within parallel operations, leading to a weaker effect on the final makespan. By contrast, the museum relies on a smaller team serving more concentrated high-demand zones. Its sweep process is therefore more dependent on longer sequential task chains and repeated transport from key locations. In this case, additional confirmation time is more likely to accumulate along the critical path, producing a stronger increase in total sweep time. These results suggest that communication efficiency is particularly important in concentrated layouts where the overall sweep is controlled by a smaller number of serially constrained operations.

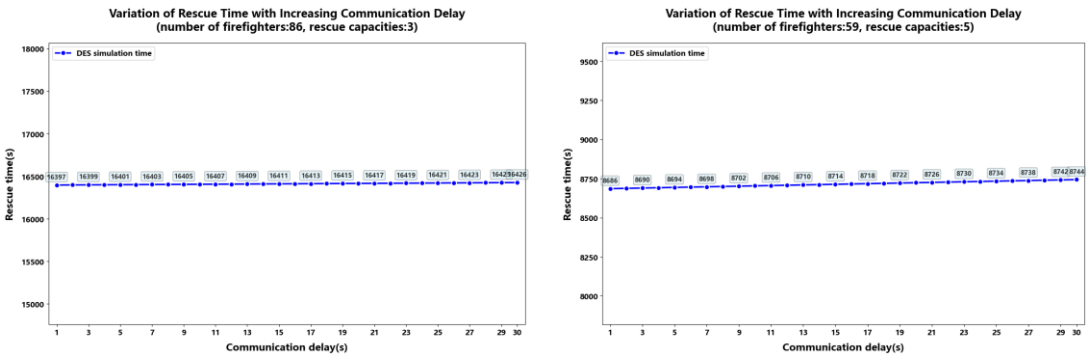

(a) Daycare center (b) Museum

Figure 8.
Impact of communication delay on rescue time.

4.4 Effects of risk-priority routing

To examine whether urgency-based task selection can improve sweep efficiency, we compared the baseline routing strategy with the risk-priority strategy described in Section 4.1. Under this setting, nodes with higher occupant load and higher predefined risk level were assigned higher priority during heuristic task selection, and the resulting plans were evaluated in the same DES framework as the baseline case.

As shown in Figure 9, risk-priority routing improves average performance in both layouts, but the magnitude and pattern of improvement differ. In the daycare center, the average sweep time decreases from 47,104.1 s to 45,553.5 s, corresponding to an overall improvement of about 3.3%. Across rescue capacities of 1, 2, and 3 persons per trip, the gains are 2.6%, 4.1%, and 3.8%, respectively. However, the fastest realized sweep time is slightly worse than that of the baseline strategy (16,421.1 s vs. 16,396.2 s), indicating that urgency-based routing mainly improves average efficiency rather than the best-case configuration.

In the museum, the average sweep time decreases from 23,605.1 s to 22,650.7 s, an overall improvement of about 4.0%. The gains by rescue capacity are 3.5%, 5.8%, and 3.5%, respectively, while the fastest sweep time remains unchanged at 8,683.6 s. This pattern suggests that risk-priority routing is particularly effective in concentrated layouts, where serving a small number of high-demand, high-risk spaces earlier can shorten the dominant rescue sequence. By contrast, in the daycare center, where high-risk demand is more spatially dispersed, the strategy still improves average performance but cannot fundamentally change the need for broad parallel coverage.

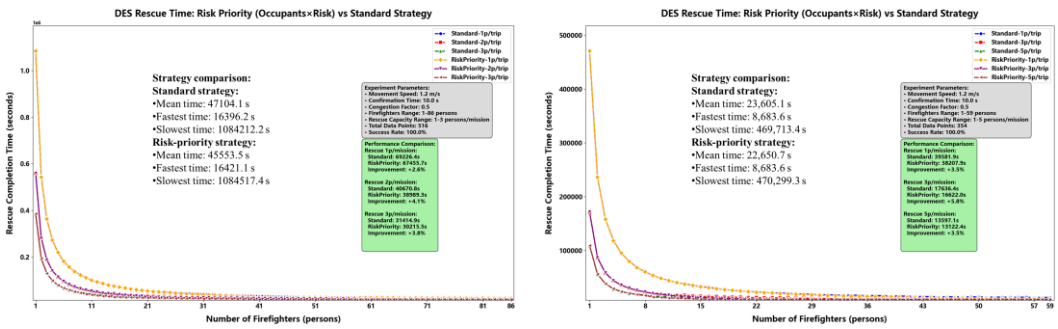

(a) Daycare center (b) Museum

Figure 9.
Comparison of total sweep time under standard and risk-priority routing.

Overall, risk-priority routing improves performance in both layouts, but its benefit is more pronounced in the museum. This suggests that prioritization is especially effective when high-risk demand is concentrated in a limited number of spatially important zones.

4.5 Effects of sensor-supported intervention

To assess the contribution of supportive technologies, we compared the baseline setting with four intervention scenarios: thermal infrared imaging (IR), indoor positioning and navigation support (POS), robotic pre-inspection (ROB), and their combined application (IR+POS+ROB). As shown in Figure 10, all interventions reduce total sweep time, but their effects differ in magnitude.

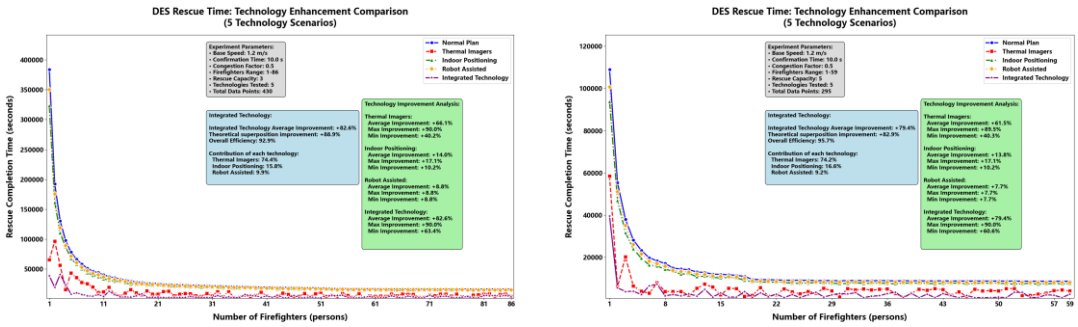

(a) Daycare center (b) Museum

Figure 10.
Effects of sensor-supported interventions on total sweep time.

Among the three individual technologies, IR produces the largest improvement in both layouts. This result suggests that reducing node-level search uncertainty is particularly effective for all-clear sweeps, where firefighters must verify multiple indoor locations under time pressure. POS provides the second-largest benefit by shortening travel time along indoor routes, while ROB yields the smallest direct reduction. Although robotic pre-inspection can reduce unnecessary checks at unoccupied nodes, its impact is more limited when most tasks are concentrated in occupied or high-priority areas.

The combined scenario achieves the greatest overall improvement, but its total benefit is smaller than the simple sum of the three individual effects. This indicates overlapping functional contributions among the technologies. In particular, once search and movement inefficiencies have already been reduced by IR and POS, the additional benefit of ROB becomes more limited.
Overall, the results show that sensor-supported interventions can improve sweep efficiency in both layouts, with the greatest gains achieved by technologies that directly reduce search and navigation uncertainty.

4.6 Integrated discussion

4.6.1 Layout-dependent sweep mechanisms

The baseline comparison shows that building layout fundamentally shapes the dominant bottleneck of all-clear sweeps. Although both layouts were evaluated under the same modeling framework, they exhibited clearly different optimal configurations and different gaps between the heuristic estimates and the DES results. This indicates that sweep efficiency is not determined by resource quantity alone, but by the interaction between spatial structure, occupant distribution, and task organization.

In the daycare center, occupants are distributed across many separate rooms, producing a dispersed service pattern. Under this condition, sweep performance depends strongly on room-level parallelism. Increasing team size therefore brings a substantial benefit because it allows more rooms to be searched and served simultaneously. By contrast, further increases in rescue capacity produce a smaller marginal gain, since the main difficulty lies not in carrying large numbers of occupants per trip, but in covering many dispersed demand locations within a limited time. This also explains why the daycare center shows a larger delay between the heuristic and DES results: more segmented circulation space and more overlapping room-to-room movements make dynamic interaction and local waiting more likely during execution.

The museum operates under a different mechanism. Occupants are concentrated in a smaller number of key exhibition areas, producing a more centralized service structure. In this case, the dominant bottleneck is repeated transport from a few high-demand locations rather than insufficient spatial coverage. As a result, rescue capacity becomes more influential than further increases in team size. The smaller DES delay in the museum further suggests that concentrated layouts with more open interior space are less sensitive to movement conflicts on shared passages. Taken together, these findings imply that all-clear sweep planning should not rely on a single deployment rule across building types; instead, the most effective resource allocation depends on whether the underlying task structure is coverage-dominated or transport-dominated.

4.6.2 Layout-dependent intervention mechanisms

The intervention analyses further show that the effectiveness of operational and technological adjustments is also layout-dependent. Communication delay increases total sweep time in both layouts, but the rate of increase differs. Under the optimal configurations, each additional second of communication delay produces an approximately 1 s increase in total sweep time in the daycare center and a 2 s increase in the museum. This difference suggests that the impact of delay is governed not simply by the number of tasks, but by whether the added delay accumulates along the critical execution path. In the daycare center, tasks are distributed across a larger firefighter team and many operations proceed in parallel, so part of the delay is absorbed within concurrent activity. In the museum, however, the sweep process relies more heavily on a smaller set of sequentially important rescue chains in concentrated zones, making the final makespan more sensitive to delayed reporting and reassignment.

A similar pattern appears in the risk-priority analysis. Prioritizing nodes with both higher risk and higher occupant load improves performance in both layouts, but the benefit is slightly larger in the museum. When demand is concentrated in a limited number of critical spaces, earlier service of those locations shortens the dominant rescue sequence more directly. In the daycare center, by contrast, the benefit is present but more moderate because high-priority demand is distributed across many separate rooms and must still be addressed through broad parallel coverage.

The sensor-supported experiments show that not all technologies contribute equally to sweep efficiency. Infrared imaging provides the largest gain in both layouts, indicating that reducing node-level search uncertainty is especially valuable in all-clear tasks. Indoor positioning offers the second-largest improvement by reducing movement inefficiency, while robotic pre-inspection provides a smaller direct effect because its main contribution lies in avoiding unnecessary checks at low-demand nodes. The combined intervention performs best overall, but its benefit is smaller than the simple sum of the individual effects,

suggesting overlapping functional contributions and diminishing marginal returns. This finding is important because it shows that technology packages should be evaluated as coordinated systems rather than as additive modules.

4.6.3 Practical implications for emergency sweep planning

These results suggest several practical implications for emergency sweep planning. First, building layout and occupant distribution should be treated as key determinants of deployment strategy. In dispersed layouts such as daycare centers, the key priority is to improve concurrent room-level coverage, which implies greater benefit from increasing team size and maintaining efficient multi-firefighter coordination. In concentrated layouts such as museums, the more effective strategy is to improve per-trip rescue throughput and reduce delays along the critical rescue chain.

Second, communication efficiency should be considered a core operational factor rather than a minor procedural detail. Even small reporting delays can propagate into meaningful increases in total sweep time, especially in layouts where execution depends on a smaller number of serially constrained operations. Third, risk-priority routing can improve performance when critical demand is spatially concentrated, suggesting that urgency-based assignment rules may be particularly useful in buildings with clear high-risk zones. Finally, sensor-supported technologies are most effective when they reduce search and navigation uncertainty, but their combined value should be assessed carefully because overlapping functions may limit additional gains.

Overall, the present findings support a planning approach in which building-specific task structure, rather than generic firefighter counts alone, guides decisions about allocation, coordination, and technology deployment.

5 Conclusion

This study proposed GMH-DES-BSM, a responder-centered graph–DES framework for evaluating all-clear building sweeps. The framework represents rooms, hallways, exits, rescue demand, verification requirements, and return-to-exit movement within a unified graph-based task structure, and uses DES to assess how candidate sweep plans perform under passage-capacity constraints and multi-firefighter interactions.

Using a two-story children's daycare center and a three-story museum as contrasting public-building layouts, the results show that sweep performance is strongly layout-dependent. Under the baseline setting, the daycare center achieved its best-performing configuration with 86 firefighters and a rescue capacity of 3 persons per trip, while the museum achieved its best-performing configuration with 59 firefighters and a rescue capacity of 5 persons per trip. The realized sweep times and the DES-based delays relative to the heuristic estimates indicate that the daycare center is more sensitive to dynamic movement interaction, whereas the museum is more strongly constrained by repeated transport from concentrated high-demand locations. This comparison suggests that layout fundamentally changes the dominant sweep bottleneck: dispersed layouts benefit more from greater parallel room-level coverage, whereas concentrated layouts benefit more from higher per-trip rescue throughput.

The scenario analyses further highlight that the effectiveness of operational adjustments and supportive technologies also depends on layout type. Communication delay increases total sweep time in both layouts, but its effect is stronger in the museum because additional confirmation time is more likely to

accumulate along a smaller number of sequentially important rescue chains. Risk-priority routing improves performance in both buildings by serving high-risk and high-demand nodes earlier, with a slightly larger gain in the museum, where critical demand is concentrated in fewer key locations. Sensor-supported interventions also reduce sweep time across both layouts. Among the tested technologies, thermal infrared imaging produces the largest improvement, followed by indoor positioning and navigation support, while robotic pre-inspection yields a smaller direct effect. The combined intervention performs best overall, but its gain is smaller than the sum of the individual effects, indicating overlapping functional contributions and diminishing marginal returns.

Overall, the study shows that efficient all-clear sweep planning should be guided by building-specific task structure rather than by generic firefighter counts alone. The main substantive contribution is the identification of layout-dependent sweep mechanisms. Dispersed multi-room layouts are primarily coverage-dominated and therefore benefit more from larger teams, while concentrated layouts are transport-dominated and benefit more from higher per-trip rescue capacity. The proposed GMH-DES-BSM framework therefore provides a practical basis for comparing candidate sweep plans, identifying effective resource-allocation strategies, and evaluating how communication and supportive technologies influence execution under different building layouts.

This study also has several limitations. First, the behavioral interaction among firefighters was simplified, and the model did not explicitly represent richer forms of coordination, adaptation, or decision revision during execution. Second, the selected building layouts were used as representative cases rather than as a comprehensive sample of public-building types. Third, the experiments assumed that a sufficiently large number of firefighters could be deployed for each sweep scenario. In practice, however, the available personnel of a responding fire department or initial dispatch team are limited, and the operational feasibility of large team configurations depends on local staffing, dispatch rules, and mutual-aid arrangements. Future work could incorporate realistic staffing constraints, staged dispatch processes, richer empirical data, additional building types, and more adaptive team coordination and re-planning mechanisms.

References

Abbas, R., & Miller, T. (2025). Exploring communication inefficiencies in disaster response: Perspectives of emergency managers and health professionals. International Journal of Disaster Risk Reduction, 120, 105393. https://doi.org/10.1016/j.ijdrr.2025.105393

Beattie, S., Xi, J. Y. S., & Chan, W. K. V. (2022). On Effective Campus Attack Response: Insights from Agent-Based Simulation for Improving Emergency Information Sharing System Design and Response Strategy. International Journal of Disaster Risk Science, 13(3), 435–447. https://doi.org/10.1007/s13753-022-00418-1

Chalmet, L. G., Francis, R. L., & Saunders, P. B. (1982). Network models for building evacuation. Fire Technology, 18(1), 90–113. https://doi.org/10.1007/BF02993491

Chen, M., Li, X., Han, D., Guo, M., Lo, J., & Liu, C. (2025). Evacuation simulation in inclined ship environment based on improved social force model. Applied Ocean Research, 154, 104415. https://doi.org/10.1016/j.apor.2025.104415

Deng, H., Ou, Z., Zhang, G., Deng, Y., & Tian, M. (2021). BIM and Computer Vision-Based Framework for Fire Emergency Evacuation Considering Local Safety Performance. Sensors, 21(11), 3851. https://doi.org/10.3390/s21113851

Fridolf, K., Andrée, K., Nilsson, D., & Frantzich, H. (2013). The impact of smoke on walking speed. Fire and Materials, 38, 725–743. https://doi.org/10.1002/fam.2217

Fridolf, K., Ronchi, E., Nilsson, D., & Frantzich, H. (2019). The representation of evacuation movement in smoke-filled underground transportation systems. Tunnelling and Underground Space Technology, 90, 28–41. https://doi.org/10.1016/j.tust.2019.04.016

Fruin, J. J. (1971). PEDESTRIAN PLANNING AND DESIGN (206 pp). Article 206 pp. https://trid.trb.org/View/114653

García-Ojeda, J. C., Bertok, B., Friedler, F., & Fan, L. T. (2013). Building-evacuation-route planning via time-expanded process-network synthesis. Fire Safety Journal, 61, 338–347. https://doi.org/10.1016/j.firesaf.2013.09.023

Ha, V., & Lykotrafitis, G. (2012). Agent-based modeling of a multi-room multi-floor building emergency evacuation. Physica A: Statistical Mechanics and Its Applications, 391(8), 2740–2751. https://doi.org/10.1016/j.physa.2011.12.034

Kobes, M., Helsloot, I., de Vries, B., & Post, J. G. (2010). Building safety and human behaviour in fire: A literature review. Fire Safety Journal, 45(1), 1–11. https://doi.org/10.1016/j.firesaf.2009.08.005

Kuligowski, E., Peacock, R., & Hoskins, B. (2010). A Review of Building Evacuation Models, 2nd Edition [Technical Note (NIST TN)]. National Institute of Standards and Technology. https://tsapps.nist.gov/publication/get_pdf.cfm?pub_id=906951

Lambert, K., Merci, B., Gryspeert, C., & Jekovec, N. (2021). Search & rescue operations during interior firefighting: A study into crawling speeds. Fire Safety Journal, 121, 103269. https://doi.org/10.1016/j.firesaf.2020.103269

Li, N., Becerik-Gerber, B., Krishnamachari, B., & Soibelman, L. (2014). A BIM centered indoor localization algorithm to support building fire emergency response operations. Automation in Construction, 42, 78–89. https://doi.org/10.1016/j.autcon.2014.02.019

Lin, J., Zhu, R., Li, N., & Becerik-Gerber, B. (2020). How occupants respond to building emergencies: A systematic review of behavioral characteristics and behavioral theories. Safety Science, 122, 104540. https://doi.org/10.1016/j.ssci.2019.104540

Muhdi, R., Gwynne, S., & Davis, J. (2009). The incorporation and validation of empirical crawling data into the buildingEXODUS model. Safety Science, 47(1), 97–104. https://doi.org/10.1016/j.ssci.2007.12.003

PAUL REVERE MUSEUM of DISCOVERY and INNOVATION. (2021). Paul Revere Memorial Museum. https://paulreveremuseum.org/wp-content/uploads/2025/02/PRMDI-MasterPlan-Final.pdf

Planning, D. and C., Missouri State University. (2024). Classroom Space Utilization Guidelines. Missouri State University. https://design.missouristate.edu/_Files/Standards/RoomLayout/ClassroomSpaceUtilizationGuidelines.pdf

Ronchi, E., & Nilsson, D. (2014). Modelling total evacuation strategies for high-rise buildings. Building Simulation, 7(1), 73–87. https://doi.org/10.1007/s12273-013-0132-9

Templeton, A., Xie, H., Gwynne, S., Hunt, A., Thompson, P., & Köster, G. (2024). Agent-based models of social behaviour and communication in evacuations: A systematic review. Safety Science, 176, 106520. https://doi.org/10.1016/j.ssci.2024.106520

Tsai, P.-F., Liao, C.-H., & Yuan, S.-M. (2022). Using Deep Learning with Thermal Imaging for Human Detection in Heavy Smoke Scenarios. Sensors, 22(14), 5351. https://doi.org/10.3390/s22145351

Vermuyten, H., Beliën, J., De Boeck, L., Reniers, G., & Wauters, T. (2016). A review of optimisation models for pedestrian evacuation and design problems. Safety Science, 87, 167–178. https://doi.org/10.1016/j.ssci.2016.04.001

Wang, M., Chen, X., & Huang, X. (2024). Robotic Firefighting: A Review and Future Perspective. In X. Huang & W. C. Tam (Eds.), Intelligent Building Fire Safety and Smart Firefighting (pp. 475–499). Springer Nature Switzerland. https://doi.org/10.1007/978-3-031-48161-1_20

Wong, M. O., & Lee, S. (2023). Indoor navigation and information sharing for collaborative fire emergency response with BIM and multi-user networking. Automation in Construction, 148, 104781. https://doi.org/10.1016/j.autcon.2023.104781

Wong, M. O., & Lee, S. (2025). Quantitative analysis of the effectiveness of real-time indoor navigation and information sharing for collaborative fire response. Developments in the Built Environment, 23, 100690. https://doi.org/10.1016/j.dibe.2025.100690

Wong, M. O., Zhou, H., Ying, H., & Lee, S. (2022). A voice-driven IMU-enabled BIM-based multi-user system for indoor navigation in fire emergencies. Automation in Construction, 135, 104137. https://doi.org/10.1016/j.autcon.2022.104137

Zhang, X., Coates, G., Dunn, S., & Hall, J. (2020). Emergency Evacuation from a Multi-floor Building using Agent-based Modeling. International Conference on Information Systems for Crisis Response and Management. https://www.semanticscholar.org/paper/Emergency-Evacuation-from-a-Multi-floor-Building-Zhang-Coates/6f37e85291bec22a43b14e6c4267d9cd8a27be44

Zhao, H., Sun, Y., Lam, C. C., Zhu, J., Pan, M., & Wong, M. O. (2025). Building Component Segmentation-oriented Indoor Localization using BIM-based Synthetic Data Generation and Deep Learning. https://doi.org/10.17863/CAM.120185

Zhu, R., Lin, J., Becerik-Gerber, B., & Li, N. (2020). Human-building-emergency interactions and their impact on emergency response performance: A review of the state of the art. Safety Science, 127, 104691. https://doi.org/10.1016/j.ssci.2020.104691